American Mineralogist, Volume 65, pages 1294–1301, 1980

Computer synthesis of optical interference figures

CRAIG M. BETHKE[1] AND RICHARD W. BIRNIE

Department of Earth Sciences, Dartmouth College
Hanover, New Hampshire 03755

Abstract

The interference figures produced by anisotropic crystals under the petrographic microscope can be synthesized by a digital model. This model allows the evaluation of a body of optical crystallographic theory as applied to interference figure phenomena. The accuracy and clarity of the figures produced by the digital model suggest applications for petrographers.

Introduction

Much of the optical theory of interference figures was developed between about 1900 and 1925 (Kamb, 1958). Research immediately preceding and during this period led to the development of three approaches to interpreting interference phenomena. The first approach involved attempts to devise a geometric model of the propagation direction of a light ray within the petrographic microscope. This approach was marked by a lengthy dispute between F. Becke and F. E. Wright in the literature during the period 1904–1923. This debate centered on the more correct construction to be used in measuring 2V from interference figures. The dispute was summarized by Wright (1923) in a paper in which he concluded that the exact construction is unknown.

The lack of an exact solution to the optical geometry of the petrographic microscope may have encouraged more general approaches. In the second approach, Michel-Levy and Lacroix (1888, p. 87–98) used a planar analog of the Biot–Fresnel Law. Michel-Levy's formula, however, was found by Wright (1907, p. 341) to give incorrect results. The third approach, known as skiodrome theory, was introduced by Becke in 1904 and developed in detail by Johannsen (1914, p. 429–440). Skiodromes became elaborately developed as a means of deriving isogyre positions. However, Kamb (1958) found that skiodromes are quantitatively and qualitatively incorrect, and he proposed alternate equations for isogyre positions in Bxa, Bxo, and ON figures.

The present research was conceived as an attempt to develop an interference figure model with the capability of quickly generating reliable images of interference figures at any crystal orientation. High-speed computer calculations permit the generation of figures without some of the simplifications employed in the hand calculations using the skiodrome or Biot–Fresnel planar analog models. The primary purpose of this model is to allow evaluation of the optical theory applied to interference figures such as that presented in commonly used optical crystallography textbooks (for example, Bloss, 1961; Stoiber and Morse, 1979).

The interference figure model, however, is useful in other applications. The orientation of an unfamiliar crystal may be determined with certainty by comparing actual interference figures with images produced by the model. Alternately, the behavior of the observed interference figure can be compared with that of the computer model as the crystal is rotated through a specific angle of stage rotation. Also, a worker might be able to identify a mineral from among several alternatives by examining the interference figure at a certain angle of stage rotation and comparing the resultant figure to the output of the digital model.

An additional application of the model is its use as a teaching aid. The use of a computer model to synthesize interference figures in a controlled situation allows a systematic approach to developing an understanding of the optical properties of crystals.

[1] Present address: Department of Geosciences, The Pennsylvania State University, University Park, Pennsylvania, 16802.

0003–004X/80/1112–1294$02.00

Theory

In this model, interference figures are considered to be produced by discrete rays of plane polarized light which conoscopically illuminate a crystal, and in the thin lens approximation (Bloss, 1961, p. 22) are transmitted to the back focal plane of the objective lens. While in a rigorous sense interference figures are formed at the focal sphere of the objective lens (Kamb, 1958), this surface can be effectively treated as a plane (Bloss, 1961, p. 111), which in a microscope is viewed through an eye piece, Bertrand lens, and analyzer. The conoscopic illumination, with a half-angle of approximately 45°, converges on a point at the center of the crystal. This point is taken as the center of the indicatrix and as the origin of the coordinate system (Fig. 1).

A vector **R** is parallel to any individual light propagation direction in the conoscopic illumination within the crystal and passes from the origin to the back focal plane of the objective lens. Vector **R′**, also passing to the back focal plane of the objective lens, corresponds to the propagation direction associated with vector **R** after refraction at the crystal–air interface. Another vector, **N**, is a special case of **R** in which **R** is parallel to the axis of the microscope. A unit vector $\hat{\mathbf{n}}$ is parallel to **N**. Vectors **H** and **V** are defined to be perpendicular to each other and to **N** and form an orthogonal vector system spanning three-space (Fig. 1). **R** and **R′**, then, may be represented as the sum of **N** and a linear combination of **H** and **V**. The crystal and, therefore, the indicatrix are held stationary in three-space. Varying the orientation of **N** has the effect of rotating the microscope about the crystal.

In constructing the model, interference figures were considered to be caused by variations in the transmitted-light intensity along different light propagation directions within the crystal. Two factors determine the fractional transmitted intensity, I/I_o, for each light propagation direction **R**. The first factor is the fractional transmitted intensity due to polarization effects of the microscope and crystal, I_p/I_o. The second factor, I_r/I_o, is the fractional transmitted intensity due to retardation within the crystal between crossed polars. While the model calculates the retardation at every point in the interference figure, the resultant interference colors cannot be displayed on a standard computer terminal.

In order to calculate I_p/I_o, the two vibration direction vectors within the crystal for a given light path **R** must be calculated. The Biot–Fresnel Law states that one of the vibration directions is the bisector of the angle produced in the plane normal to **R** at the origin by the intersection of that plane with the two planes each containing an optic axis and the propagation direction **R** (Fig. 2). The other vibration direction is the vector normal to the first vibration direction and normal to **R**. These crystal vibration directions are always the major and minor axes of the elliptical section of the indicatrix in the plane passing through the origin and normal to **R** (Bloss, 1961, p. 160). The vibration directions associated with the major and minor axes are referred to as $\mathbf{V}_1$ and $\mathbf{V}_2$, respectively.

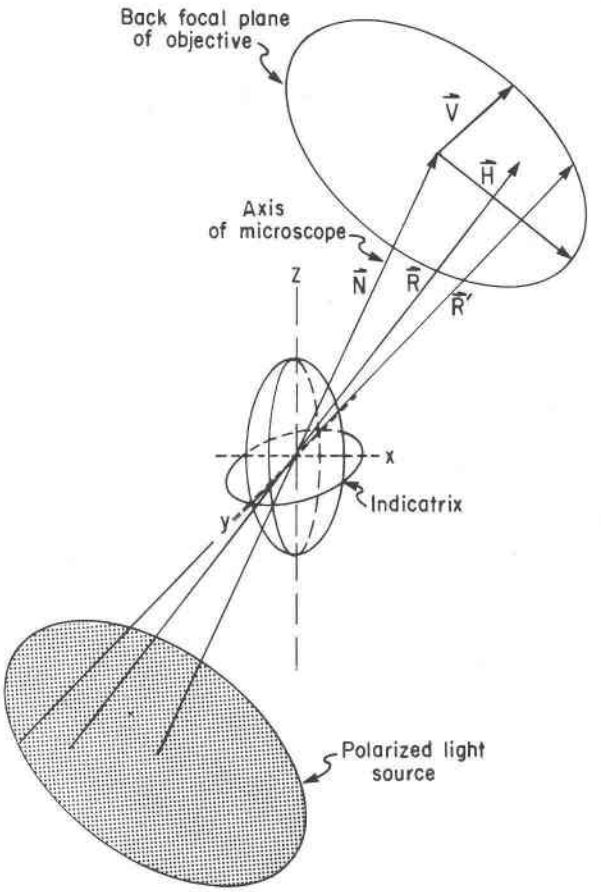

Fig. 1. Schematic representation of model. **R** represents a propagation direction of convergent light within the crystal, and **R′** represents the propagation direction corresponding to **R** after refraction at the crystal–air interface. **R** and **R′** pass from the origin to the back focal plane of the objective lens. **N** is a special case of **R** in which **R** is parallel to the axis of the microscope. The origin of the indicatrix is located within the crystal and the indicatrix is fixed in 3-space.

The surface of the indicatrix of a crystal with indices of refraction α, β, and γ is an ellipsoid whose locus of points (x, y, z) satisfies the equality

$$x^2/\alpha^2 + y^2/\beta^2 + z^2/\gamma^2 = 1$$

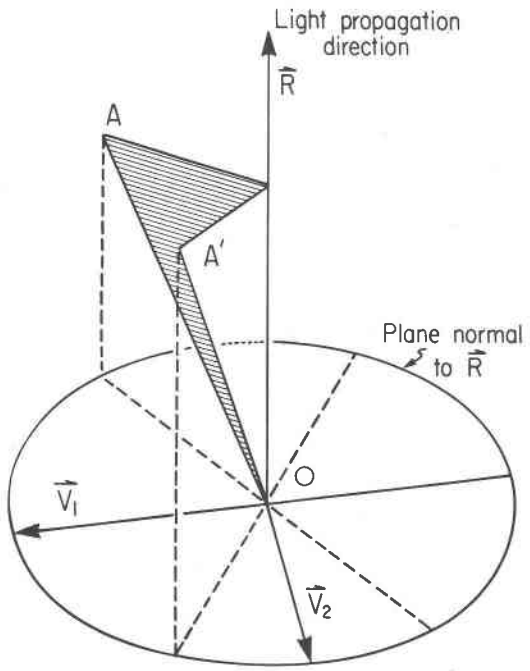

Fig. 2. The Biot–Fresnel Law. Segments OA and OA′ are optic axes of the crystal, and $\mathbf{V}_1$ and $\mathbf{V}_2$ are the resultant vibration directions associated with the light propagation direction within the crystal, **R**. $\mathbf{V}_1$ and $\mathbf{V}_2$ are the major and minor axes of the elliptical section of the indicatrix in the plane normal to **R** (after Stoiber and Morse, 1979, p. 162).

Knowing this relation and the orientation of a light propagation direction within the crystal, **R**, which, after refraction, passes to a point on the back focal plane of the objective lens, the vibration direction vectors $\mathbf{V}_1$ and $\mathbf{V}_2$ may be calculated by an iterative technique. The technique solves for the vectors of greatest and least length from the origin to the indicatrix surface in the plane of the indicatrix section normal to **R**.

Specifically, an arbitrary vector **h**, with components (h_1, h_2, h_3), from the origin and perpendicular to **R** is found by solving for a non-trivial solution to the equation

$$\mathbf{h} \cdot \mathbf{R} = 0$$

This vector may be scaled so that it passes from the origin to the surface of the indicatrix by the factor, s:

$$s = (h_1^2/\alpha^2 + h_2^2/\beta^2 + h_3^2/\gamma^2)^{-1/2}$$

The vector **h** is rotated in incremental steps through an arc of 180° so that it is always contiguous with the surface of the indicatrix and is always perpendicular to **R**. The vectors $\mathbf{V}_1$ and $\mathbf{V}_2$ are taken to be the value of the vector **h** at its greatest and least lengths, respectively.

In order to calculate I_p/I_o, $\mathbf{V}_1$ and $\mathbf{V}_2$ are projected onto a plane normal to the axis of the microscope (Fig. 3). The fractional transmitted intensity of the analyzer is resolved in this plane. Since $\hat{\mathbf{n}}$, the unit vector parallel to **N**, is of unit length and normal to this plane, the lengths of the components of the vibration direction vectors which are parallel to the axis of the microscope, c_1 and c_2, may be calculated as the dot products of the vibration directions with the unit normal:

$$c_1 = \mathbf{V}_1 \cdot \hat{\mathbf{n}}$$

$$c_2 = \mathbf{V}_2 \cdot \hat{\mathbf{n}}$$

The projections of $\mathbf{V}_1$ and $\mathbf{V}_2$ onto the plane normal to the axis of the microscope are designated $\mathbf{v}_1$ and $\mathbf{v}_2$, respectively, and are calculated as:

$$\mathbf{v}_1 = \mathbf{V}_1 - c_1\hat{\mathbf{n}}$$

$$\mathbf{v}_2 = \mathbf{V}_2 - c_2\hat{\mathbf{n}}$$

In the general case, the fractional transmitted intensity due to polarization effects along a propagation direction of polarized light with vibration direction, **P**, passing through a polarizing substance with

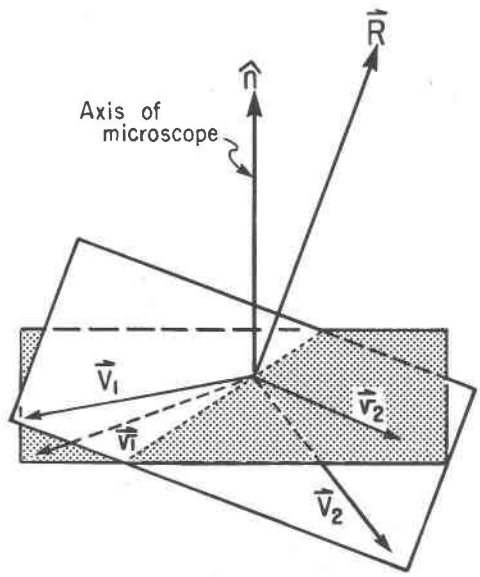

Fig. 3. Projection of crystal vibration directions onto the plane normal to the axis of the microscope. $\mathbf{V}_1$ and $\mathbf{V}_2$ are the vibration directions corresponding to light propagation direction **R** and are contained in the plane normal to **R** (unshaded). $\mathbf{v}_1$ and $\mathbf{v}_2$ are projections of $\mathbf{V}_1$ and $\mathbf{V}_2$ onto the plane which is normal to the axis of the microscope (stippled).

allowed vibration direction, $\mathbf{v}$, at angle ϕ to $\mathbf{P}$ is given by Malus' Law (Tipler, 1976, p. 625):

$$I_p/I_o = \cos^2\phi$$

This angle may be calculated from the definition of the dot product:

$$\cos\phi = \mathbf{v} \cdot \mathbf{P}/|\mathbf{v}||\mathbf{P}|$$

where $|\mathbf{v}|$ is the length of $\mathbf{v}$, and $|\mathbf{P}|$ is the length of $\mathbf{P}$.

In a petrographic microscope, a ray of polarized light is first resolved into the allowed vibration directions of the crystal and then resolved by the analyzer. If a crystal had one vibration direction, Malus' Law would be compounded to:

$$I_p/I_o = \cos^2\phi \cos^2(\pi/2 - \phi)$$
$$= \cos^2\phi (1 - \cos^2\phi)$$

where ϕ is the angle between the vibration direction of the polarized light and the crystal vibration direction, and $(\pi/2 - \phi)$ is the angle between the crystal vibration direction and the allowed vibration direction of the analyzer. Since uniaxial and biaxial crystals have two vibration directions, $\mathbf{v}_1$ and $\mathbf{v}_2$ at angles ϕ_1 and ϕ_2 from the polarizer-allowed vibration direction, respectively, Malus' Law becomes:

$$I_p/I_o = \cos^2\phi_1 (1 - \cos^2\phi_1) + \cos^2\phi_2 (1 - \cos^2\phi_2)$$

The remaining factor, the fractional transmitted intensity due to retardation effects, I_r/I_o, is readily approximated. Since the lengths of $\mathbf{V}_1$ and $\mathbf{V}_2$ represent the high and low indices of refraction, n_1 and n_2, for the light propagation direction considered, the retardation, Δ, for a given $\mathbf{R}$ is:

$$\Delta = t(n_1 - n_2)|\mathbf{R}|/|\mathbf{N}|$$

where t is the thickness of the crystal along $\mathbf{N}$ and the ratio $|\mathbf{R}|/|\mathbf{N}|$ accounts for increased path lengths through the crystal for light propagation directions not parallel to the axis of the microscope.

For a given retardation along a light propagation direction, the fractional transmitted intensity due to retardation effects for monochromatic light of wavelength λ is given in Johannsen (1914, p. 345–346):

$$I_r/I_o = \sin^2(\pi\Delta/\lambda)$$

Integration of this equation over visible wavelengths, however, is time-consuming. An approximation of the value of I_r/I_o as a function of retardation with a crystal thickness of 30 μm was obtained from linear approximations over 3 ranges of retardation:

$$I_r/I_o = 0 \qquad \Delta < 10$$
$$I_r/I_o = 0.006\,(\Delta - 10) \qquad 10 \le \Delta \le 176$$
$$I_r/I_o = 1 \qquad 176 < \Delta$$

where Δ is expressed in nanometers. Since change in light perception by the human eye under normal conditions is a logarithmic function of change in light intensity, the Fechner–Weber Law (Baird and Noma, 1978, p. 78), deviations from this approximation at high fractional intensities are negligible.

Thus the total fractional transmitted intensity for a given light propagation direction through a crystal is the product of the fractional transmitted intensities due to polarization and to retardation:

$$I/I_o = I_p/I_o \cdot I_r/I_o$$

The highest possible value of I/I_o, with $\phi_1 = \phi_2 = \pi/4$ and $I_r/I_o = 1$, is one quarter the intensity of the light ray at the light source, or one half the intensity of the polarized light incident to the crystal. Values of less than 1% of the incident polarized light are taken to be dark areas of the computed interference figure; values of greater than 1% are considered to appear light to the eye.

It is possible to apply more sophisticated optical theory to the model. For example, the effects of surface reflection, multiple internal reflection, refraction at other surfaces, and light absorption by the crystal, mount, and microscope are not considered. Also, the geometry of the microscope, especially the objective lens, is somewhat simplified. These effects, however, are not expected to have a significant impact on the interference figures produced by the model. Kamb (1958) describes the effects of the rotation of the plane of polarization by refraction at the surfaces of the converging and objective lenses, but notes that these effects tend to cancel each other.

Since the model calculates the retardation of all points in the interference figure, the computer program could be used to produce interference figures in color. This would have the added advantages of showing isochromes and the effects of any actual or hypothetical accessory plates on the figures produced. This modification has not been employed because the necessary color graphics have not been available to the project.

The small amount of computer memory required by the vector techniques employed in this model allows its adaptation to the inexpensive minicomputers becoming available on the market.

Application

In the model developed, the only input necessary for the computer synthesis of interference figures is

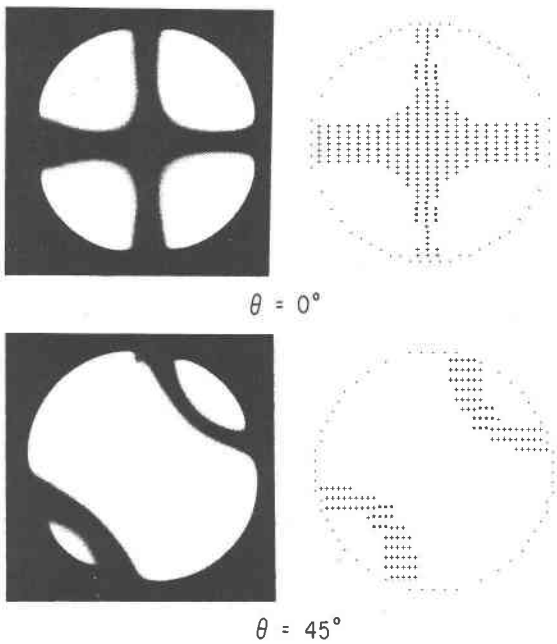

Fig. 4. Photomicrographs (left column) of barite Bxa figures at various angles of stage rotation (θ) starting at the crossed position with the trace of the optic plane oriented north–south and computer-generated figures (right column) produced using the indices of refraction of barite at the same angles of stage rotation.

the refractive indices of the crystal under consideration, a vector describing the orientation of the crystal on the microscope stage, and the angle of rotation of the stage, θ, from an arbitrary initial position. On subsequent program runs, the refractive indices and orientation vector need not be supplied if these values have not changed since the previous program run.

To facilitate the use of the program at a variety of terminals and on a variety of computer systems, interference figures are represented by character matrix plots. Blanks in the matrix plot represent points in the figure where more than 1% of the light intensity incident to the crystal is transmitted to the eyepiece. Plus signs represent points at which less than 1% of the incident light is transmitted, that is points that appear dark to the eye. An asterisk marks a point of very low retardation ($\Delta < 10$ nm), and identifies the region of the melatopes, if they appear in the field of view.

The theory described was evaluated by generating interference figures that were based on the optical properties of real minerals. In every case, the synthesized interference figures behaved as actual interference figures behave. Figure 4 is a comparison of

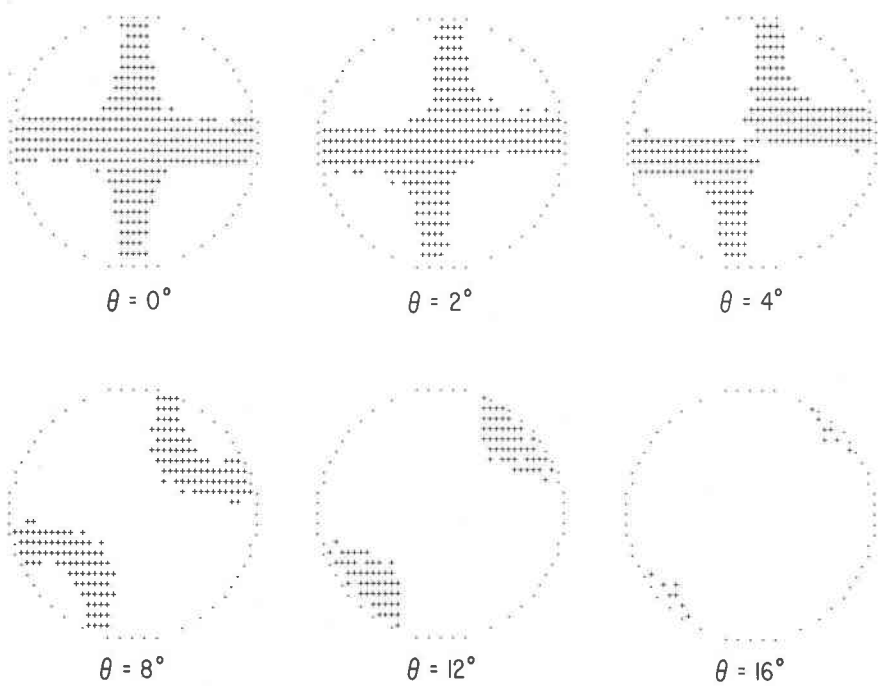

Fig. 5. Computer-generated albite Bxa figures at various angles of clockwise stage rotation (θ) from an initial crossed position.

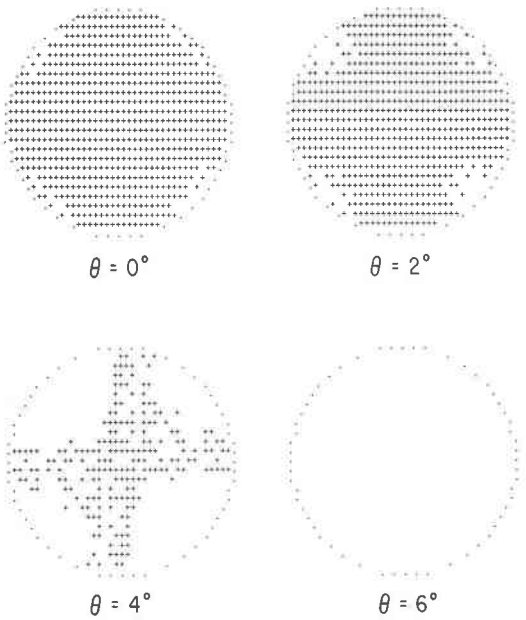

Fig. 6. Computer-generated albite ON (flash) figures at various angles of clockwise stage rotation (θ).

computer-generated figures calculated using the optical properties of barite and actual barite Bxa figures.

Figure 5 is a sequence of Bxa figures calculated for a crystal of albite. The Z (Bxa) indicatrix axis is normal to the plane of the microscope stage, and the stage is being rotated clockwise. Initially, the X (Bxo) axis runs north–south, and the Y (ON) axis runs east–west. Because $2V_Z$ exceeds about 65°, the melatopes are out of the field of view. As the stage is rotated, the cross breaks up into hyperbola-shaped isogyres which leave the field of view at about 16° of stage rotation.

Figure 6 is a sequence of optic normal (ON) or flash figures for albite. At an angle of rotation of 4°, the figure begins to break up. While the scattered pattern of blanks and plus signs at this angle of rotation represents rounding and incremental "step function" error in the last decimal places of the numerical values used in the digital techniques, it is an accurate reflection of the fuzziness of the interference figure. At a rotation angle of 6°, the isogyres have completely disappeared. Contrast this with the Bxa figure (Fig. 5) rotated through these angles.

As an example of an application of a detailed knowledge of interference figures, Figure 7 juxtaposes Bxa figures of the biaxial negative feldspar minerals, orthoclase ($2V_x = 60°$) and anorthite ($2V_x = 77°$). Before rotation, the figures are similar, except that the orthoclase melatopes lie within the field of view. The position of the melatopes is, of course, not discernible in actual Bxa figures at the crossed position. As the stage is rotated, the anorthite cross breaks up more quickly than the orthoclase cross. At

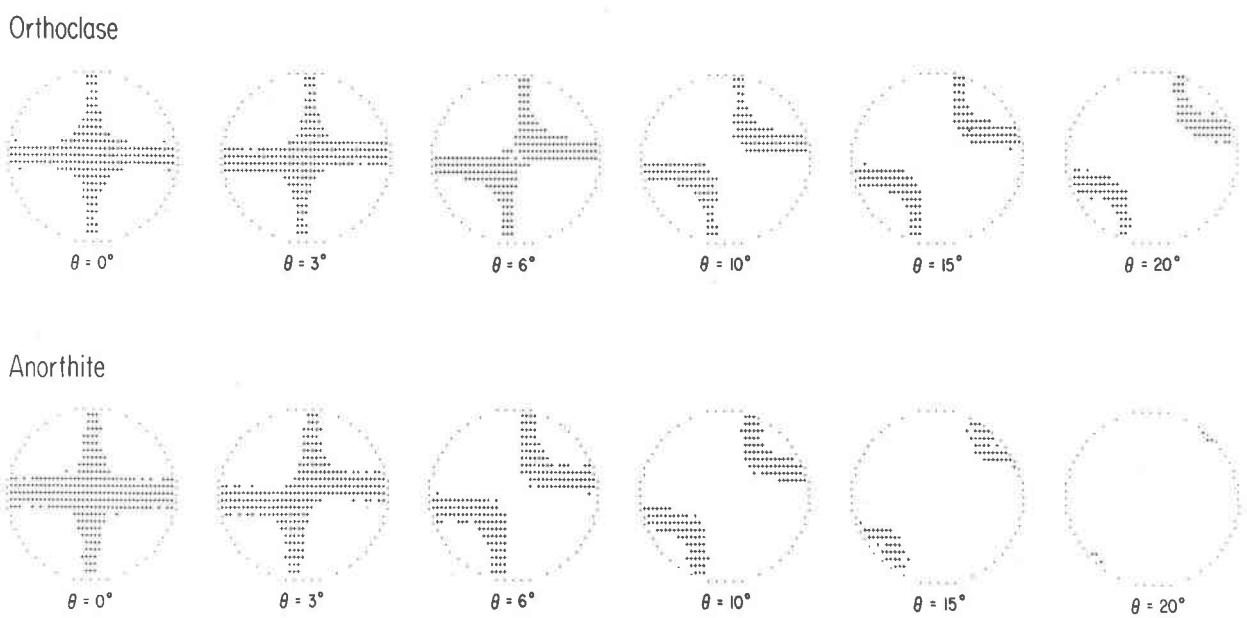

Fig. 7. Computer-generated Bxa figures for orthoclase (top row) and anorthite (bottom row) through clockwise stage rotation (θ).

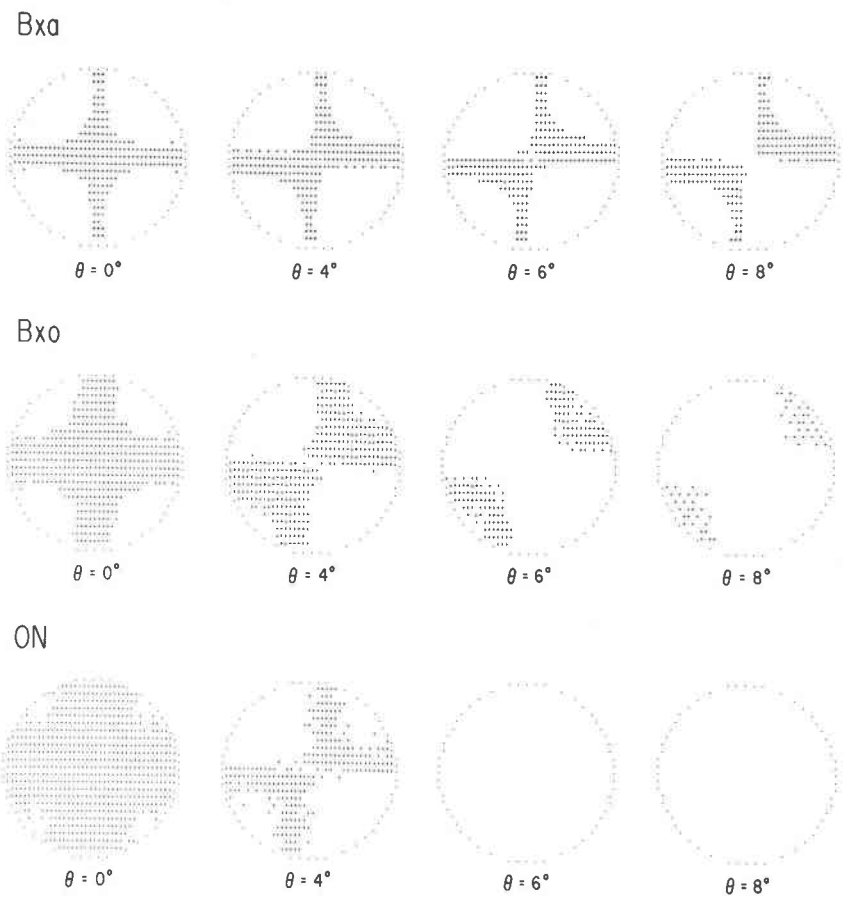

Fig. 8. Computer-generated orthoclase Bxa (top row), Bxo (center row), and ON (bottom row) figures through clockwise stage rotation (θ).

6° of rotation, the orthoclase figure still retains its cross configuration, while the anorthite figure has clearly broken into two distinct isogyres. The anorthite isogyres finally leave the field of view at about 20°, while the orthoclase isogyres remain visible throughout the stage rotation. The possibility exists, therefore, of differentiating from among optically similar minerals quickly and easily through the comparison with the output of the digital model.

Figure 8 shows the relationship of orthoclase Bxa, Bxo, and ON (flash) figures through equal angles of stage rotation. As the stage is rotated, the ON figure breaks up almost immediately; the Bxa and Bxo break up more slowly. At 6° rotation, the Bxa figure still has not broken into isogyres; the Bxo figure has broken into isogyres which are about to leave the field of view; and the ON figure has disappeared completely. This sequence suggests that interference figures produced by orthoclase in a petrographic microscope may be immediately differentiated by simply rotating the stage 6°. The importance of rotation angles in differentiating interference figures is discussed by Kamb (1958).

The model, of course, is not restricted to producing two-isogyre figures of biaxial crystals. Figure 9 is a figure calculated for a crystal of topaz, the Z axis of which is rotated from the vertical (parallel to the microscope axis) in both the X and Y directions. This represents the most general case of interference figures where no principal axes of the indicatrix are parallel to the microscope stage.

Conclusions

This study has demonstrated that by the application of conventional optical theory the computer synthesis of petrographic microscope interference figures is possible. Only refractive index and crystal orientation data are necessary input. The behavior of the computer-generated interference figures matches the behavior of actual interference figures well

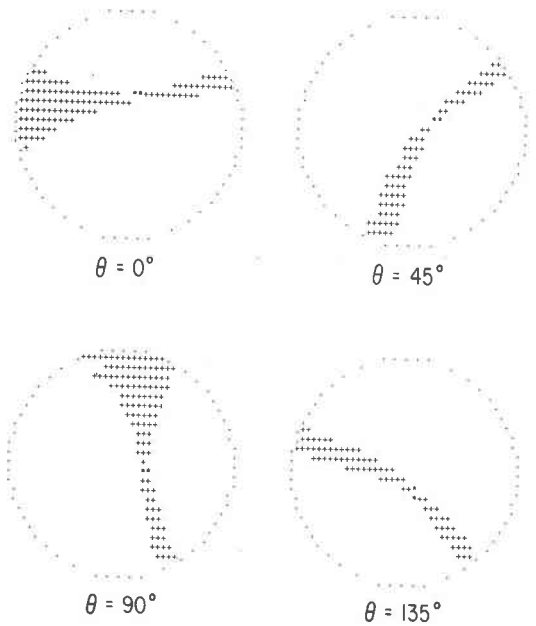

Fig. 9. Computer-generated topaz one-isogyre figures. The Z (Bxa) indicatrix axis has been rotated away from the microscope axis in both the X (Bxo) and Y (ON) directions. Note that while the stage (and the melatope in the field of view) is rotated clockwise, the isogyre rotates counterclockwise.

enough to be useful in the laboratory or classroom environment. Further, the model allows the evaluation of commonly presented optical theory of the origin of interference figure phenomena with the conclusion that the optical theory is valid, at least to the resolution of the model. More detailed optical theory may be applied to the model, but this would not have a significant influence on the figures produced.

Copies of the program written in Fortran IV may be obtained by writing the authors.

Acknowledgments

Computer support for the project was provided by Dartmouth College Computing and additional support was provided by the Department of Earth Sciences, Dartmouth College. John B. Lyons and John M. Hughes, Dartmouth College, and F. Donald Bloss, Virginia Polytechnic Institute and State University, reviewed the manuscript.

References

Baird, J.C. and E. Noma (1978) *Fundamentals of Scaling and Psychophysics.* Wiley, New York.

Bloss, F.D. (1961) *An Introduction to the Methods of Optical Crystallography.* Holt, Rinehart, and Winston, New York.

Johannsen, A. (1914) *Manual of Petrographic Methods,* 1st ed. McGraw-Hill, New York.

Kamb, W.B. (1958) Isogyres in interference figures. *Am. Mineral., 43,* 1029–1067.

Michel-Levy, A. and A. Lacroix (1888) *Les Mineraux des Roches.* Librairie Polytechnique, Baudry, Paris.

Stoiber, R.E. and S.A. Morse (1979) *Microscopic Identification of Crystals.* Krieger, Huntington, New York.

Tipler, P.A. (1976) *Physics.* Worth Publishers, New York.

Wright, F.E. (1907) The measurement of the optic axial angle of minerals in the thin section. *Am. J. Sci., 174,* 317–369.

——— (1923) The formation of interference figures, a study of the phenomena exhibited by transparent inactive crystal plates in convergent polarized light. *J. Opt. Soc. Am., 7,* 779–817.

Manuscript received, March 4, 1980;
accepted for publication, May 8, 1980.